Chapter 2
Quantum Chromodynamics

The Standard Model of Particle Physics (SM) embodies our knowledge of the strong and electroweak interactions. It contains as fundamental degrees of freedom the spin-$\frac{1}{2}$ quarks and leptons, the spin-1 gauge bosons, and the spin-0 Higgs field. Despite the presence of a number of *a-priori* unknown parameters, this model is a mathematical construction of considerable predictive power. Notably, it suggested the existence of the W and Z bosons, the gluon, and the top and charm quarks before these particles were observed. In 2013, the particle content of the SM was made complete by the experimental discovery of the Higgs Boson [1, 2].

Here we focus on the strong-force component of the SM, which specifies how quarks and gluons bind together to form ordinary hadronic matter. This is the theory of Quantum Chromodynamics (QCD), describing all strong-interaction physics at all distance scales, from high energy particle collisions and the decay of heavy nuclei to the properties of matter under extreme conditions such as in the core of a neutron star. This diverse physics is encapsulated in a single formula of alluring simplicity: the Lagrangian of QCD. Despite its apparently simple form, deriving the physical dynamics of a system from this equation poses a tremendous theoretical challenge.

Asymptotic freedom—the property that quarks and gluons interact very weakly in high-energy reactions—ensures that perturbative approaches can be applied to QCD at small distance scales. In this way one can obtain precise theoretical predictions from the SM which may be rigorously tested through high-energy scattering experiments. In the low-energy regime, however, the QCD coupling is large and perturbative techniques cannot be used. The only known first-principles approach to QCD at these scales is numerical: a discretised form of the QCD equations can be solved exactly, using supercomputers, on a finite four-dimensional grid representing space-time. This technique is named lattice QCD.

Of course, although we receive invaluable insight by discretising QCD, we have also lost direct comparison with the physical, continuous, world. To be able to compare the results of lattice QCD simulations with experiment, one must extrapolate to the physical point. Precisely, the continuum limit (as lattice spacing $a \to 0$), the infinite volume limit (as lattice size $L \to \infty$), and, as computation time often

P.E. Shanahan, *Strangeness and Charge Symmetry Violation in Nucleon Structure*, Springer Theses, DOI 10.1007/978-3-319-31438-9_2

limits simulations to larger-than-physical quark masses, the continuation into small quark masses $\left(\text{as } m_q \to m_q^{(\text{phys.})}\right)$ must be taken. This final limit, the so-called chiral extrapolation, is arguably the most difficult of the three to implement and will be a particular focus of this body of work.

As technological and algorithmic advances now allow lattice simulations to be performed near, or even at, the physical quark masses, it is foreseeable that chiral extrapolation as a means of reaching the physical point will soon become obsolete. With this in mind, we explore this technique not only as an essential link between lattice simulations and Nature, but as an invaluable tool with which to develop a deeper understanding of QCD from unphysical test cases which cannot be explored experimentally. As we will see in later chapters, one can extend chiral extrapolation techniques to isolate vacuum-quark effects, explore the quark-mass dependence of observables and hence extract mass-derivative quantities, and extend SU(2)-flavour–symmetric simulations to the SU(2)-broken world. Combining the insight afforded by unphysical lattice simulations with experimental results allows one to deduce hard-to-calculate quantities to a precision that is yet unreachable by direct computation. In this way, we set the benchmarks for the next generation of experimental tests of the SM.

After outlining the mathematical formulation of QCD in the next section, we briefly discuss the numerical lattice QCD approach. The remainder of this chapter is devoted to the concepts of strangeness and charge symmetry violation in the nucleon, which are the core themes of this body of work.

2.1 Mathematical Formulation

Mathematically, QCD is a gauge field theory describing the interactions of 'colour-charged' particles. It is based on the non-Abelian, compact, and simple Lie group SU(3), commonly represented by the group of 3×3 complex unitary matrices with unit determinant. The gluons A_μ arise as the (spin-1) gauge bosons of this theory. As such, they may be identified with the generators of SU(3) rotations in colour-space[1], $A_\mu = t_a A_\mu^a$, and transform in the adjoint representation of the gauge group. The dimension of the adjoint representation (equal to the number of generators) is $3^2 - 1 = 8$ for SU(3), thus the gluons are colour-octet. The quark fields ψ are spin-$\frac{1}{2}$ fermions in the fundamental representation of the gauge group and carry colour and flavour labels. The dimension of the fundamental representation is the degree of the group, $N = 3$ for SU(3), so the quarks are colour-triplet.

The classical, unrenormalised Lagrangian density of QCD is completely specified by the conditions of renormalisability and invariance under the SU(3) gauge transformations

[1]Here $t_a = \lambda_a/2$, where λ_a, $a = 1, \ldots, 8$ are the Gell-Mann matrices with normalisation $\text{Tr}(\lambda_a \lambda_b) = \delta_{ab}$.

$$\psi(x) \to \psi'(x) = U(x)\psi(x), \tag{2.1a}$$

$$A_\mu(x) \to A'_\mu(x) = U(x)A_\mu(x)U^{-1}(x) + \frac{i}{g}\left(\partial_\mu U(x)\right)U^{-1}(x), \tag{2.1b}$$

where $U(x) = \exp\left(i\phi^a(x)t^a\right)$ defines an independent SU(3) transformation at every point in space-time. Neglecting a quark-mass mixing phase—the θ parameter associated with the strong CP problem—as it is known to be extremely small [3], one finds[2]

$$\begin{aligned}\mathcal{L}_{\text{QCD}} &= \sum_q \overline{\psi}_q^i \left(i\gamma^\mu D_\mu^{ij} - \delta^{ij} m_q\right)\psi_q^j - \frac{1}{4}F_{\mu\nu}^{(a)}F^{(a)\mu\nu} \\ &= \overline{\psi}\left(i\not{D} - M_q\right)\psi - \frac{1}{4}F_{\mu\nu}F^{\mu\nu}.\end{aligned} \tag{2.2}$$

The second line shows the standard compact notation—fundamental-representation colour indices i, j, adjoint-representation colour indices a, and flavour labels $q = u, d, s, \ldots$ have been suppressed. The Dirac matrix γ^μ, where μ is a Lorentz vector index, expresses the vector nature of the strong force, and the non-zero quark masses are encoded in $M_q = \text{diag}(m_u, m_d, m_s \ldots)$. There is no gauge-invariant way of including a gluon mass. The QCD covariant derivative introduces the coupling g of the quarks to the gluons:

$$D_\mu^{ij} = \delta^{ij}\partial_\mu - igt_a^{ij}A_\mu^a, \tag{2.3}$$

and the non-Abelian gluon field strength tensor is given by

$$F_{\mu\nu}^{(a)} = \partial_\mu A_\nu^a - \partial_\nu A_\mu^a + gf_{abc}A_\mu^b A_\nu^c, \tag{2.4}$$

where f_{abc} are SU(3) Lie group structure constants. This is non-linear in terms of the gauge field and as a result the gluon kinetic energy term of the Lagrangian generates three and four-gluon self-interactions. These interactions are responsible for many of the salient features of QCD.

In particular, because of the gluon self-coupling, the polarisation of virtual gluons in the vacuum antiscreens (i.e., enhances) colour charge. This effect dominates over the screening effect of the quark vacuum-polarisation, which is analogous to that of QED. As a result, the QCD coupling, $\alpha_s = g^2/4\pi$, runs to become small at large scales; at high energy QCD is essentially a theory of free partons—quarks and gluons—which only interact through relatively small quantum corrections that can be systematically, perturbatively, calculated. This is the property of asymptotic freedom, for which Politzer, Gross, and Wilczek were awarded the 2004 Nobel Prize [4, 5].

[2] Counterterms and ghost and gauge-fixing terms are implicit; they are all unnecessary for the lattice QCD approach which we will consider here.

In contrast, at low energies accelerators reveal a particle spectrum which bears no resemblance to the non-interacting theory: free quarks are never observed. Instead, towers of strongly-bound colour-singlet particles named hadrons emerge. This is termed confinement and is understood as a consequence of the property that the force between two colour-charges does not diminish as they are separated. Instead, linear string-like potentials build up between partons. These strings only 'break' when the energy contained is large enough to create an additional quark-antiquark pair out of the vacuum. As a result, one only observes mesons, which have the quantum numbers of a quark-antiquark pair, and baryons, with the quantum numbers of three quarks. The properties of these hadrons are the focus of this body of work.

Analytic derivations of hadron properties have proven to be impossible except in some extreme limiting cases; at the relevant low energy scales the strong coupling becomes large and perturbation theory is no longer valid. While many models and approximations are used to study low-energy processes: the limit of the large number of colours; generalisations of the original Shifman-Vainshtein-Zakharov sum rules; QCD vacuum models and effective string models; the AdS/CFT conjecture; and Schwinger-Dyson equations, the only known way to study QCD in the nonperturbative regime directly is to use numerical methods. As suggested earlier, the most successful of these, and the only one rigorously derived from the fundamental theory, is lattice QCD.

2.2 Lattice Quantum Field Theory

First proposed by Wilson in 1974 [6], lattice QCD is a first-principles method of calculating QCD observables numerically. In short, a discretised version of the full QCD theory is solved explicitly on a four-dimensional lattice of points (3 space, 1 time dimension). Any such lattice is characterised by a finite lattice spacing a which is not physical but acts as a method of regularisation. The limit $a \to 0$ must be taken to connect to the physical theory.

As the only known direct probe of QCD in the nonperturbative regime, the lattice is an important source of information for tests of the SM; it provides results for various low-energy hadronic matrix elements that are complimentary to those obtained using phenomenological approaches. It has also become a viable framework for calculations of nuclear few-body quantities [7, 8], and for the exploration of part of the QCD phase diagram [9, 10]. As we will see in later chapters, a great advantage of lattice field theory is that the technique allows precise control over the parameters of QCD. By varying these parameters one may probe more than QCD at the physical point—for example, one can 'turn off' vacuum loop contributions or change the quark masses—to develop a deeper understanding of nonperturbative phenomena. In this section we introduce the basic concepts and terminology relevant to lattice QCD. A comprehensive summary of the approach may be found in Refs. [11–13].

2.2.1 The Discretised Action

Lattice gauge theory is based on the Feynman path integral approach to quantum field theory [14]. In this formulation of QCD, observables are given by the expectation values of field operators. These expectation values, known as Green's functions, can be expressed as functional derivatives of the generating functional,

$$\mathcal{Z}_{\mathrm{QCD}} = \int \delta A_\mu \, \delta\overline{\psi} \, \delta\psi \, e^{iS_{\mathrm{QCD}}}, \tag{2.5}$$

with respect to the various sources. If all Green's functions could be calculated, QCD would be solved. In Minkowski space, however, this formulation of QCD does not lend itself to numerical computation because of the complex term $e^{iS_{\mathrm{QCD}}}$ which appears in Eq. (2.5); the oscillatory integrand causes cancellations between different regions of phase space. For this reason lattice QCD is formulated in Euclidean space-time. The partition function

$$\mathcal{Z}^E_{\mathrm{QCD}} = \int \delta A_\mu \, \delta\overline{\psi} \, \delta\psi \, e^{-S_{\mathrm{QCD}}} \tag{2.6}$$

is obtained by a Wick rotation ($t \to -it_E$) of the corresponding expression in Minkowski space (Eq. (2.5)). This form allows a probabilistic interpretation of the functional integral; the exponential factor corresponds exactly to the Boltzmann weighting of a statistical ensemble.

In this section we describe the construction of a discretised lattice action for QCD:

$$S_{\mathrm{QCD}} = S_F[U, \psi, \overline{\psi}] + S_G[U], \tag{2.7}$$

where the subscripts F and G denote the fermion and purely-gauge components, respectively.

2.2.1.1 Fermions

In Euclidean space-time the Dirac action for a free fermion is written as

$$\int d^4x \, \overline{\psi}(x) \left(\not{D} + m\right) \psi(x). \tag{2.8}$$

In the discretised theory the quark fields $\psi(n)$ reside on the sites n of the lattice, i.e., the fermionic degrees of freedom are

$$\psi(n), \quad \overline{\psi}(n), \quad n \in \Lambda. \tag{2.9}$$

We will restrict ourselves to four-dimensional cubic lattices:

$$\Lambda = \left\{ x \in \mathbb{R}^4 \middle| x = an,\ n \in \mathbb{Z}^4 \right\}, \tag{2.10}$$

where a is the discrete lattice spacing. While this is the standard topology, others have been explored [15, 16] and there has been a recent resurgence of interest in anisotropic lattices [17, 18]. In practice, of course, the lattices used for numerical simulations have some finite extent. As in the continuum theory, the spinors ψ carry colour, flavour, and Dirac indices (which are suppressed in our notation).

The derivative in Eq. (2.8) may be discretised using a symmetrised finite difference, where appropriate gauge links are included to maintain gauge invariance:

$$\overline{\psi} \not{D} \psi \to \sum_{\mu=1}^{4} \overline{\psi} \gamma_\mu \nabla_\mu \psi = \frac{1}{2a} \overline{\psi}(n) \sum_{\mu=1}^{4} \gamma_\mu \left[U_\mu(n)\, \psi(n+\hat{\mu}) - U_\mu^\dagger(n-\hat{\mu})\, \psi(n-\hat{\mu}) \right], \tag{2.11}$$

where the gauge fields $U_\mu(n)$ are elements of the gauge group SU(3). These fields are oriented and attached to the links of the lattice: $U_\mu(n)$ lives on the link connecting the sites (n) and $(n+\hat{\mu})$. Under a gauge transformation $\lambda(n)$,

$$U_\mu(n) \to \lambda(n)\, U_\mu(n)\, \lambda(n + a\hat{\mu})^{-1}. \tag{2.12}$$

Finally, implementing the discretisation of the integral in Eq. (2.8) as a sum over the set of space-time points Λ, we arrive at the 'naive' action for fermions in an external gauge field U:

$$\begin{aligned} S_F^{\mathrm{N}}[U, \psi, \overline{\psi}] &= \sum_{n \in \Lambda} \overline{\psi}(n) \left(\frac{1}{2a} \sum_{\mu=1}^{4} \gamma_\mu \left[U_\mu(n)\, \psi(n+\hat{\mu}) - U_\mu^\dagger(n-\hat{\mu})\, \psi(n-\hat{\mu}) \right] + m\psi(n) \right) \\ &= \sum_{n,m \in \Lambda} \overline{\psi}(n)\, M_{nm}^{\mathrm{N}}[U]\, \psi(m), \end{aligned} \tag{2.13}$$

where M^{N} is the naive interaction matrix

$$M_{nm}^{\mathrm{N}}[U] = m\, \delta_{nm} + \frac{1}{2a} \sum_{\mu=1}^{4} \gamma_\mu \left[U_{n\mu}\, \delta_{n(m-\mu)} - U_{(n-\mu)\mu}^\dagger\, \delta_{n(m+\mu)} \right]. \tag{2.14}$$

By Taylor-expanding U_μ and ψ in powers of the lattice spacing a, one can see that the naive fermion action has $\mathcal{O}(a^2)$ errors. It is clear, however, that the first-order derivative can only couple lattice sites separated by $2a$. As a result, certain high-momentum modes do not correspond to a large value of the action. This leads to unwanted additional long-range degrees of freedom called doublers; in the continuum limit there are $2^d = 16$ flavours of quark rather than one.

There are two common methods of fixing the doubling problem. The first reduces the number of doublers by 'staggering' the quark degrees of freedom on the lattice.

This procedure is described in Ref. [11]. The other technique, which is used in this work, involves adding additional operators to the quark action (which scale with a and so vanish in the continuum limit) to suppress the doublers by driving them to higher energies.

Precisely, the Wilson term—a particular (energy) dimension-five operator—is added to the standard naive lattice fermion action, giving the 'Wilson action':

$$S_F^{\mathrm{W}}[U,\psi,\overline{\psi}] = \sum_{n\in\Lambda}\overline{\psi}(n)\left[\sum_{\mu=1}^{4}\left(\gamma_\mu\nabla_\mu - \frac{1}{2}ra\Delta_\mu\right) + m\right]\psi(n). \tag{2.15}$$

Here ∇ denotes the finite difference defined in Eq. (2.11), and the operator Δ removes the unwanted doublers by coupling adjacent lattice sites:

$$\Delta_\mu\psi(n) = \frac{1}{a^2}\left[U_\mu(n)\,\psi(n+\hat{\mu}) + U_\mu^\dagger(n-\hat{\mu})\,\psi(n-\hat{\mu}) - 2\psi(n)\right]. \tag{2.16}$$

In terms of link variables, the Wilson action is written as

$$S_F^{\mathrm{W}}[U,\psi,\overline{\psi}] = \sum_{n,m\in\Lambda}\overline{\psi}^L(n)\,M_{nm}^{\mathrm{W}}[U]\,\psi^L(m),$$

where

$$aM_{nm}^{\mathrm{W}}[U] = \delta_{nm} - \kappa\sum_{\mu=1}^{4}\left[(r-\gamma_\mu)\,U_{n\mu}\,\delta_{n(m-\mu)} + (r+\gamma_\mu)\,U_{(n-\mu)\mu}^\dagger\,\delta_{n(m+\mu)}\right], \tag{2.17}$$

with a field renormalisation

$$\kappa = 1/(2ma+8r), \tag{2.18}$$

$$\psi^L = \psi/\sqrt{2\kappa}. \tag{2.19}$$

It is typical to take $r=1$.

In the continuum limit it is clear that, through the addition of the Wilson term, we have introduced $\mathcal{O}(a)$ discretisation errors into the fermion matrix; the Dirac action of Eq. (2.8) becomes

$$\int d^4x\,\overline{\psi}(x)\left(\not{D} + m - a\frac{r\not{D}^2}{2}\right)\psi(x) + \mathcal{O}\left(a^2\right). \tag{2.20}$$

Numerical simulations using Wilson fermions must thus be performed on very fine lattices, which are computationally expensive, in order for continuum extrapolations to be reliable. It has become standard to improve the uncertainties of the Wilson action through the addition of higher-dimension operators. This procedure is known as the Symanzik improvement program [19].

We discuss here only one choice of improved fermion action, which we use in this work (see Chap. 7). The Sheikholeslami-Wohlert fermion action [20] includes the so-called 'clover' term—a gauge-invariant, local, dimension-five operator—in addition to the standard terms of the Wilson action:

$$S_F^{\mathrm{SW}}[U,\psi,\overline{\psi}] = S_F^{\mathrm{W}}[U,\psi,\overline{\psi}] - \frac{a\, c_{\mathrm{SW}}\, r}{4} \sum_{n\in\Lambda} \sum_{\mu,\nu=1}^{4} \overline{\psi}(n)\, \sigma_{\mu\nu}\, F_{\mu\nu}(n)\, \psi(n). \tag{2.21}$$

Here c_{SW} is the clover coefficient which can be tuned (typically nonperturbatively using the axial Ward identity [21]) to remove all $\mathcal{O}(a)$ artefacts. Further details may be found in Refs. [11–13].

2.2.1.2 Gluons

The matrix-valued link variable $U_\mu(x)$ was introduced in Eq. (2.11) to maintain the gauge-invariance of the covariant derivative. Based on its gauge transformation properties (Eq. (2.12)), we interpret $U_\mu(n)$ as a lattice version of the gauge transporter connecting the points (n) and $(n+\hat{\mu})$. Under this identification, we can express the link variable in terms of the algebra-valued continuum gauge field $A_\mu(x)$:

$$U_\mu(n) = \mathcal{P} \exp ig \int_0^a A_\mu(n+\lambda\hat{\mu}) d\lambda, \tag{2.22}$$

where the operator $\mathcal{P}$ path-orders the A_μ along the integration path and g is the coupling constant.

From Eq. (2.12) it is clear that the trace over a closed (Wilson) loop of link variables is a gauge-invariant object. Various such loops are used in combination to build the lattice version of the QCD gauge action—the precise construction is arbitrary provided that the usual continuum action is recovered in the $a \to 0$ limit. It is natural to consider the simplest case first; the shortest nontrivial closed loop on the lattice is the so-called plaquette, constructed by the product of four links enclosing an elementary square:

$$P_{\mu\nu}(n) = \mathrm{Re}\,\mathrm{Tr}\left[U_{\mu(n)}\, U_\nu(n+\hat{\mu})\, U_\mu^\dagger(n+\hat{\nu})\, U_\nu^\dagger(n)\right]. \tag{2.23}$$

Using Eq. (2.22), and expanding the integral, we express $P_{\mu\nu}$ in terms of the field A_μ:

$$\begin{aligned} P_{\mu\nu}(n) &= \mathrm{Re}\,\mathrm{Tr}\,\mathcal{P} e^{ig \oint_{\square_n} A\cdot dx} \\ &= \mathrm{Tr}\,\mathcal{P}\left[1 - \frac{1}{2}\left(g \oint_{\square_n} A\cdot dx\right)^2 + \mathcal{O}(A^4)\right]. \end{aligned} \tag{2.24}$$

Stoke's theorem gives an expression for the integral:

$$\begin{aligned}\oint_{\square_n} A \cdot dx &= \int_0^a dx_\mu dx_\nu \left[\partial_\mu A_\nu(n+x) - \partial_\nu A_\mu(n+x)\right] \\ &= \int_0^a dx_\mu dx_\nu F_{\mu\nu}(n+x) \\ &= a^2 F_{\mu\nu}(n) + \frac{a^4}{24}\left(\partial_\mu^2 + \partial_\nu^2\right) F_{\mu\nu}(n) + \mathcal{O}\left(a^6, A^2\right), \end{aligned} \tag{2.25}$$

where the last line follows from a Taylor expansion of $F_{\mu\nu}(n+x)$ about the lattice site (n). Substituting this expression back into Eq. (2.24), the plaquette term becomes

$$P_{\mu\nu}(n) = 1 - \frac{1}{2} g^2 a^4 \mathrm{Tr}\left[F_{\mu\nu}(n)^2\right] + \mathcal{O}\left(g^2 a^6, a^8, g^4 a^6\right). \tag{2.26}$$

This expansion yields the 'Wilson action' for gluons on the lattice:

$$\begin{aligned} S_G^{\mathrm{W}}[U] &= \frac{2}{g^2} \sum_{n\in\Lambda} \sum_{\mu<\nu} \left[1 - P_{\mu\nu}(n)\right] \\ &= \frac{a^4}{2g^2} \sum_{n\in\Lambda} \sum_{\mu<\nu} \mathrm{Tr}\left[F_{\mu\nu}(n)^2\right] + \mathcal{O}\left(a^2, a^2 g^2\right). \end{aligned} \tag{2.27}$$

This expression differs from the continuum gluon action by terms which are $\mathcal{O}(a^2)$ and $\mathcal{O}(a^2 g^2)$. These artefacts can be removed, however, by adding other Wilson loops to the action which have different errors at $\mathcal{O}(a^2)$. For example, the Lüscher-Weisz gauge action [22] includes 1×2 rectangular loops and parallelogram-shaped loops as well as the standard plaquette:

$$S_G^{\mathrm{LW}}[U] = \frac{2}{g^2}\left(c_0 \sum_{\text{plaq.}} \left[1 - P_{\mu\nu}\right] + c_1 \sum_{\text{rect.}} \left[1 - R_{\mu\nu}\right] + c_2 \sum_{\text{par.}} \left[1 - L_{\mu\nu}\right]\right), \tag{2.28}$$

where $R_{\mu\nu}$ and $L_{\mu\nu}$ denote products of gauge links, enclosing 1×2 rectangles and parallelograms respectively, defined analogously to $P_{\mu\nu}$ in Eq. (2.23). The relative weighting coefficients c_i (that are generically functions of g^2) are chosen to satisfy $c_0 + 8c_1 + 8c_2 = 1$, which ensures that discretisation errors are cancelled to $\mathcal{O}(a^4)$. Two common choices of the weighting coefficients are the Iwasaki gauge action [23] and the tree-level improved action [24] which we use in Chap. 7. This latter choice sets $c_0 = 20/12$, $c_1 = -1/12$, and $c_2 = 0$.

2.2.2 Lattice Expectation Values

Physical observables are calculated in the lattice approach as expectation values:

$$\langle \mathcal{O} \rangle = \frac{1}{\mathcal{Z}} \int \delta A_\mu \, \delta\overline{\psi} \, \delta\psi \, \mathcal{O} \, e^{-S_{\mathrm{QCD}}}, \tag{2.29}$$

where $\mathcal{O}$ can be any combination of operators expressed in terms of time-ordered products of gauge and quark fields, and $\mathcal{Z}$ is the Euclidean–space-time partition function (Eq. (2.6)). One can remove any dependence of $\mathcal{O}$ on the quark fields as dynamical variables by performing Wick contractions to re-express them in terms of propagators. The propagators, for a given background field U, are determined by inverting the Dirac operator. In terms of an interaction matrix M (e.g., Eq. (2.14) or (2.17)),

$$S_f(m, n, U) = (M[U]^{-1})_{nm} \tag{2.30}$$

gives the amplitude for the propagation of a quark from site (n) to site (m) (where the spin-colour indices are suppressed). Now, integrating over the fermion field (recalling that the fermion action is given by $S_F = \overline{\psi} M \psi$, Eq. (2.13)),

$$\langle \mathcal{O} \rangle = \frac{\int \delta A_\mu \det[M] \, \mathcal{O} \, e^{-S_G}}{\int \delta A_\mu \det[M] \, e^{-S_G}}. \tag{2.31}$$

As the gauge group SU(3) is continuous, there are infinitely many gauge configurations that contribute to this expression. For this reason the integral over the gauge fields is approximated statistically:

$$\langle \mathcal{O} \rangle \approx \frac{1}{N} \sum_{i=1}^{N} \mathcal{O}\left(U^{[i]}\right). \tag{2.32}$$

Here $\mathcal{O}(U^{[i]})$ is the operator $\mathcal{O}$ evaluated for the i^{th} field configuration $U^{[i]}$ of an ensemble of N such configurations which have been randomly generated based on the acceptance probability of the weight function $\det[M[U]]e^{-S_{G[U]}}$. This generation is performed iteratively using a Markov process; beginning from an initial configuration $U^{[0]}$, a chain of configurations $\left\{U^{[1]}, U^{[2]}, \ldots\right\}$ is generated using a Monte-Carlo–style algorithm satisfying

$$P\left(U^{[i-1]} \to U^{[i]}\right) P\left[U^{[i-1]}\right] = P\left(U^{[i]} \to U^{[i-1]}\right) P\left[U^{[i]}\right], \tag{2.33}$$

where $P\left(U \to U'\right)$ is the transition probability between configurations U and U'. General criteria exist that guarantee that the configurations visited are indeed distributed according to the desired probability distribution after a sufficient number of iterations.

The generation of gauge configurations is computationally expensive. The cost of calculating the fermion determinant $\det[M[U]]$ depends not only on the number of configurations generated, but on the number of lattice sites, the lattice volume, and the quark masses. Because of the sheer size of the fermion matrix M, its determinant is approximated numerically. This is done using iterative algorithms which involve inverting matrices that become progressively more singular as the quark masses become lighter. Similarly, the quark propagators, which must be calculated explicitly for each gauge configuration, become more expensive to calculate at light masses. Moreover, the lattice volume required becomes increasingly large. For this reason calculations at or near the physical masses are only now becoming tractable [25].

A further cost-saving approximation is that quark propagators are typically calculated from a fixed source point to every other point on the lattice; 'all-to-all' propagators from every lattice site to every other site are simply too expensive. As a result, contributions to observables from quark-line–disconnected loops—which could appear at any point on the lattice—are neglected in most simulations (see Sect. 2.3.1). The effects of this omission in the case of baryon electromagnetic form factors will be discussed in detail in Chap. 7.

2.2.3 Scale Setting

A characteristic of lattice simulations is that all quantities are calculated in units of the unknown lattice spacing a, which must be determined by matching an observable to its physical value[3]. This can be done in a variety of ways. Two common methods, often referred to as the 'mass-independent' and 'mass-dependent' scale-setting schemes, are of particular interest to us here:

1. **Mass-independent.** The inverse bare coupling β determines the lattice spacing a. That is, simulations at some fixed value of β are extrapolated to the physical point (usually linearly in the bare quark mass $am_{q_{\text{sea}}}$), and the value of some observable at that point is used to set the common scale a for *all* lattice ensembles at that common β.
2. **Mass-dependent.** The lattice spacing varies with bare quark mass. That is, a is determined separately for each set of bare parameters $(\beta, am_{q_{\text{sea}}})$ by using a physical observable that is assumed to be independent of the quark masses. A typical choice of observable is the Sommer scale, r_0, which is related to the force between static quarks at relatively short distance, or any of a range of similar quantities.

We could think of these two choices of scale-setting prescription as different ways of absorbing the observed quark-mass dependence of the ratio r_0/a at fixed β.

[3]The lattice spacing is not physical, but acts as a method of regularisation. The only physical quantities are mass-ratios.

Method 1 essentially assumes that this dependence may be attributed to the variation of r_0 with quark mass, while method 2 instead assumes that a is changing. What is not often considered is that both r_0 and a may have some dependence on the sea-quark mass, which would lead to an intermediate scale in some sense. Such a 'mixed' scale-setting procedure would be nontrivial to implement.

Of course, in the continuum limit, and after the chiral extrapolation to physical quark masses has been performed, the results of each method of scale setting must agree for physical observables. When considering quantities which are expressed as derivatives with respect to quark mass, however, the choice of scale-setting method becomes far more significant; these quantities, by the very definition of the derivative, depend on the scale away from the physical point and hence on the scale-setting scheme chosen. This distinction will be particularly relevant to the discussion of Chap. 5, where we calculate the octet baryon sigma terms as derivatives via the Feynman-Hellmann theorem.

2.3 Strangeness and Charge Symmetry Violation in the Nucleon

We finish this chapter with an introduction to the concepts of strangeness and charge symmetry violation (CSV) in nucleon structure; these topics are the unifying themes of this body of work. Both strange and CSV observables are associated with deviations from approximate features of the nucleon in QCD. They are hence benchmark quantities for modern precision tests of the theory.

In particular, strange nucleon observables occupy a position of comparable importance in QCD to that of the Lamb shift in the history of QED. While lattice QCD and models have described a number of valence-quark–dominated hadronic properties extremely accurately [26], strange observables can only arise through quantum fluctuations of the vacuum in which a strange-antistrange quark pair briefly bubble into and out of existence. The calculation of such quantities directly within QCD, and their verification by experiment, is thus the ideal test of our understanding of virtual sea quarks in the nucleon.

Charge symmetry, defined formally in Sect. 2.3.2, is related in QCD to the near mass-degeneracy of the u and d quarks. At the quark level this symmetry is, of course, very badly broken, but this is hidden by dynamical chiral symmetry breaking; in nuclear reactions charge symmetry holds to better than about 1% [27]. Precise calculations of CSV observables therefore also provide SM benchmarks for tests of QCD. In our discussion, the themes of strangeness and CSV are connected through the electromagnetic form factors (Chap. 7); the strange quark and CSV contributions to these quantities cannot be distinguished experimentally.

2.3.1 Nucleon Strangeness

The net strangeness of the nucleon is, of course, zero; its quantum numbers correspond to those of two u quarks and a single d. In QCD, however, these light valence quarks are accompanied by a fluctuating sea of all flavours of $q\overline{q}$ pairs. The magnitude of the vacuum contributions to observables from different flavours scales with quark mass. Clearly, the lightest non-valence quark flavour—the s for the nucleon—will provide the dominant vacuum contribution, and hence be the most interesting phenomenologically.

Other than the valuable information about the quantum vacuum which strange observables provide in their own right, these quantities are also relevant in other arenas. Most importantly, the strange nucleon sigma terms (Chap. 5) are essential input for the interpretation of dark matter direct-detection experiments. In general, however, the uncertainties in both experimental and theoretical determinations of the strangeness matrix elements, including the strange sigma terms, are large. Clearly lattice QCD promises significant improvement by facilitating the calculation of definitive quantitative results for these observables.

The challenge in determining strange nucleon observables in lattice QCD lies in the evaluation of the so-called disconnected insertions, illustrated in Fig. 2.1(a). Determining these terms explicitly requires the calculation of all-to-all propagators—from every point on the lattice to every other point—which is prohibitively expensive compared to the evaluation of the connected insertions. Consequently, there are very few lattice calculations of disconnected observables [28, 29]. In these studies the all-to-all propagators are stochastically estimated. For these reasons, the lattice QCD simulations which we use and develop in this body of work will include only connected insertions. We emphasise here that this does *not* omit the entire meson cloud of QCD. This distinction is illustrated explicitly in Fig. 2.2.

We investigate the role of strange quarks in generating different nucleon observables by combining connected-only lattice QCD simulations, chiral effective field theory, and experimental input; the aim is to build a cohesive picture of the contribution not only from the strange quark, but from the dynamical vacuum more generally, in QCD. In particular, we investigate the strange nucleon sigma terms (Chap. 5) and the strange contribution to the electromagnetic form factors of the nucleon (Chap. 7).

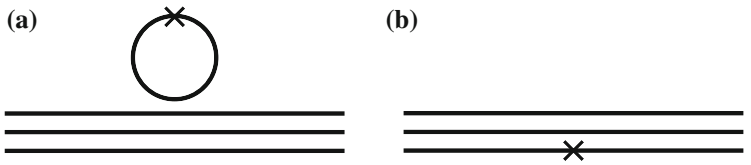

Fig. 2.1 Quark-line 'skeleton' diagrams showing connected and disconnected insertions of some operator (represented by the crossed vertex). All gluons and additional (spectator) quark-antiquark pairs are omitted for clarity, (**a**) Disconnected insertion, (**b**) Connected insertion

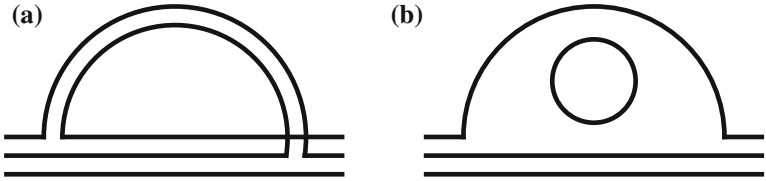

Fig. 2.2 Quark-line 'skeleton' diagrams showing the meson cloud contributions to hadronic observables. All gluons and additional quark-antiquark pairs are omitted for clarity. Any operator insertion into a connected quark line (i.e., any line other than the vacuum bubble in Fig. 2.2(b)) is included in a connected-only calculation, (**a**) Quark-line connected meson loop, (**b**) Quark-line disconnected meson loop

2.3.2 Charge Symmetry Violation

Charge symmetry is formally defined as the invariance of the strong interaction under an isospin rotation exchanging u and d quarks; it corresponds precisely to a rotation by π about the '2' axis in isospin space (compared to isospin symmetry, which is invariance under an arbitrary rotation in this space). The violation of this symmetry is arguably small: the proton-neutron mass difference is one part in a thousand [30] and many nuclear reactions proceed identically if protons and neutrons are interchanged. The effects of this small CSV, however, may be hugely significant. For example, if the proton-neutron mass difference were reversed, protons could undergo beta decay, atoms such as carbon, the building block of all organic matter, could not form, and life as we know it would be impossible. CSV also explains the discrepancy between the calculated and measured binding energy differences of mirror nuclei (Okamoto-Nolen-Schiffer anomaly [31]) and may play a role in precision tests of the SM [32], including those at the LHC [33].

In lattice QCD studies, however, the small effects of CSV are in general ignored; it is standard to perform '2+1-flavour' simulations where the light quarks are mass-degenerate. A full '1+1+1-flavour'—isospin-broken—study would involve a significantly more complicated tuning procedure in order to find the lattice parameters corresponding to the close-to-physical space of interest. With the majority of lattice simulations not yet at the physical average light-quark mass, the effect of CSV has thus long been a secondary concern; only very recently have lattice studies been performed that partially (for the valence quarks only) [34] or fully [35] include strong CSV contributions.

CSV effects have also, until very recently [36–38], been neglected in many standard analyses of experimental results. For example, the assumption of good charge symmetry at the parton level has been applied to global fits of parton distribution functions to experimental data [33, 39] in order to reduce the number of independent functions by a factor of two. Experimental tests of the SM are now, however, reaching a level of precision where CSV effects may be important. For example, it has been suggested [40] that CSV artefacts could significantly reduce the 3-sigma discrepancy with the SM value for the weak mixing angle found by

the NuTeV collaboration [41] in neutrino-nucleus deep inelastic scattering. For this reason, we devote considerable attention to the role of CSV in the nucleon (returning to a discussion of the NuTeV anomaly in Chap. 6).

In future chapters we combine 2+1-flavour lattice QCD simulations with input from chiral effective field theory to determine CSV effects in a number of nucleon observables. In particular, we separate the strong and electromagnetic contributions to the proton-neutron mass difference (Chap. 4), as well as determining the level of CSV in the baryon sigma terms (Chap. 5), and in moments of parton distribution functions (Chap. 6). In Chap. 7 we describe the first lattice-QCD–based calculation of the CSV electromagnetic form factors and, importantly, present the remarkable result that these quantities are constrained to be an order of magnitude smaller than previous best estimates. This revelation paves the way for a new generation of experimental determinations of the strange nucleon form factors to constrain these quantities to an unprecedented level of precision. Moreover, because of the extremely small SM background, measurements of CSV in the electromagnetic form factors may in the future provide some insight in searches for new physics.

References

1. G. Aad et al. (ATLAS Collaboration), Phys. Lett. **B716**, 1 (2012)
2. S. Chatrchyan et al. (CMS Collaboration), Phys. Lett. **B716**, 30 (2012)
3. C.A. Baker et al., Phys. Rev. Lett. **97**, 131801 (2006)
4. D.J. Gross, F. Wilczek, Phys. Rev. Lett. **30**, 1343 (1973)
5. H.D. Politzer, Phys. Rev. Lett. **30**, 1346 (1973)
6. K.G. Wilson, Phys. Rev. D **10**, 2445 (1974)
7. T. Inoue et al. (HAL QCD Collaboration), Phys. Rev. **C91**, 11001 (2015)
8. H. Nemura, (HAL QCD Collaboration), Int. J. Mod. Phys. **E23**, 1461006 (2014)
9. C.S. Fischer, J. Luecker, C.A. Welzbacher, Phys. Rev. D **90**, 034022 (2014)
10. P. de Forcrand, J. Langelage, O. Philipsen, W. Unger, Phys. Rev. Lett. **113**, 152002 (2014)
11. H.J. Rothe, World Sci. Lect. Notes Phys. **74**, 1 (2005)
12. J. Smit, Cambridge Lect. Notes Phys. **15**, 1 (2002)
13. C. Gattringer, C.B. Lang, Lect. Notes Phys. **788**, 1 (2010)
14. R.P. Feynman, Rev. Mod. Phys. **20**, 367 (1948)
15. W. Celmaster, Phys. Rev. D **26**, 2955 (1982)
16. N.H. Christ, R. Friedberg, T.D. Lee, Nucl. Phys. B **202**, 89 (1982)
17. R. Morrin, A.Ó. Cais, M. Peardon, S.M. Ryan, J.-I. Skullerud, (TrinLat Collaboration), Phys. Rev. **D74**, 014505 (2006)
18. R.G. Edwards, B. Joó, H.-W. Lin, Phys. Rev. D **78**, 054501 (2008)
19. K. Symanzik, Nucl. Phys. B **226**, 187 (1983)
20. B. Sheikholeslami, R. Wohlert, Nucl. Phys. B **259**, 572 (1985)
21. N. Cundy et al., Phys. Rev. D **79**, 094507 (2009)
22. M. Lüscher, P. Weisz, Commun. Math. Phys. **97**, 59 (1985)
23. S. Itoh, Y. Iwasaki, Y. Oyanagi, T. Yoshié, Phys. Lett. B **148**, 153 (1984)
24. W. Bietenholz et al., Phys. Rev. D **84**, 054509 (2011)
25. S. Dürr et al., Phys. Lett. B **701**, 265 (2011)
26. S. Dürr et al., Science **322**, 1224 (2008)
27. G.A. Miller, A.K. Opper, E.J. Stephenson, Ann. Rev. Nucl. Part. Sci. **56**, 253 (2006)
28. A. Abdel-Rehim et al., Phys. Rev. D **89**, 034501 (2014)

29. T. Doi et al., Phys. Rev. D **80**, 094503 (2009)
30. J. Beringer et al., Particle data group. Phys. Rev. D **86**, 010001 (2012)
31. J.A. Nolen, J.P. Schiffer, Ann. Rev. Nucl. Part. Sci. **19**, 471 (1969)
32. R. Horsley et al., Phys. Rev. D **83**, 051501 (2011)
33. J.T. Londergan, J.C. Peng, A.W. Thomas, Rev. Mod. Phys. **82**, 2009 (2010)
34. S. Borsanyi et al. (BMW Collaboration), Phys. Rev. Lett. **111**, 252001 (2013)
35. S. Borsanyi et al. (BMW Collaboration), [arXiv:1406.4088]
36. A.D. Martin, R.G. Roberts, W.J. Stirling, R.S. Thorne, Eur. Phys. J. C **35**, 325 (2004)
37. E.N. Rodionov, A.W. Thomas, J.T. Londergan, Mod. Phys. Lett. A **9**, 1799 (1994)
38. E. Sather, Phys. Lett. B **274**, 433 (1992)
39. J.T. Londergan, A.W. Thomas, Prog. Part. Nucl. Phys. **41**, 49 (1998)
40. J.T. Londergan, A.W. Thomas, Phys. Lett. B **558**, 132 (2003)
41. G.P. Zeller et al. (NuTeV Collaboration), Phys. Rev. Lett. **88**, 091802 (2002)

http://www.springer.com/978-3-319-31437-2

Strangeness and Charge Symmetry Violation in Nucleon Structure

Shanahan, P.E.

2016, XV, 213 p. 58 illus., 19 illus. in color., Hardcover
ISBN: 978-3-319-31437-2